Highly efficient bacterial removal and disinfection by magnetic barium phosphate nanoflakes with embedded iron oxide nanoparticles

Journal:	*Environmental Science: Nano*
Manuscript ID	EN-ART-04-2018-000403
Article Type:	Paper
Date Submitted by the Author:	12-Apr-2018
Complete List of Authors:	song, junyi; National University of Defense Technology, College of Science; University of California Santa Barbara, Institute for Collaborative Biotechnologies Zhang, Fan; Nanjing Agricultral University, College of Sciences; University of California Santa Barbara, Bren School of Environmental Science and Management HUANG, Yuxiong; University of California, Santa Barbara, Bren School of Environmental Science and Management Keller, Arturo; University of California, Santa Barbara, Bren School of Environmental Science and Management Tang, Xiaoxiu; Nanjing Agricultural University Zhang, wanning; Shanghai Jiao Tong University Jia, weibin; Nanjing Agricultural University Santos, Jerome; University of California, Santa Barbara

Environmental Significance Statement

Contamination of drinking water with bacteria is a persistent public health problem around the world. We developed a novel magnetic barium phosphate nanoflake material (FBP) for efficient bacterial removal and disinfection of drinking water. FBP exhibits much higher removal efficiency than comparable materials (nano and convential). Importantly, it has potential for microbe control even in high salinity conditions (e.g. treated effluent). FBP can maintain a high bacterial removal efficiency after being reused for five cycles. Several types of forces and mechanisms were also discussed in detail. This work represents a key advance towards the facile synthesis and viable application of magnetic nanocomposites in treating water with high microbial contamination.

Highly efficient bacterial removal and disinfection by magnetic barium phosphate nanoflakes with embedded iron oxide nanoparticles

Junyi Song [a, b, ‡], *Fan Zhang* [c, d, ‡, *], *Yuxiong Huang* [d], *Arturo A. Keller* [d], *Xiaoxiu Tang* [c], *Wanning Zhang* [e], *Weibin Jia* [f], *Jerome Santos* [b]

a College of Science, National University of Defense Technology, Changsha 410073, China

b Institute for Collaborative Biotechnologies, University of California, Santa Barbara, CA 93106, USA.

c College of Sciences, Nanjing Agricultural University, Nanjing 210095, PR China.

d Bren School of Environmental Science and Management, University of California, Santa Barbara, CA 93106, USA.

e School of Chemistry and Chemical Engineering, Shanghai Jiao Tong University, Shanghai 200240, PR China.

f College of Life Sciences, Nanjing Agricultural University, Nanjing 210095, PR China.

‡ These authors contributed equally.

* Corresponding Author (Fan Zhang): Tel & Fax: 86-25-84396098; E-mail: zhangfan0128@njau.edu.cn

Abstract Magnetic barium phosphate nanoflakes with embedded iron oxide nanoparticles, Fe_3O_4@$Ba_3(PO_4)_2$ (denominated FBP), were prepared through a facile and inexpensive two-step process. FBP was used to purify water heavily contaminated with *E. coli* (initial concentration of 5×10^8 CFU/mL). FBP exhibited high removal efficiency (97%) within 30 min at 25 ^oC and pH 6. We investigated the effects of factors such as pH, ionic strength, co-existing anions, temperature, contact time, material dosage, and initial concentration of bacterial suspension, and developed optimized treatment conditions. The negligible effect of solution ionic strength on bacterial removal efficiency of FBP indicates its potential for microbial control even in high salinity water. Importantly, FBP can maintain a high bacterial removal efficiency of 87% after being reused for five cycles. FBP's magnetic properties allow an easy recovery from water. Several types of forces and mechanisms are thought to be involved in the bacterial removal process by FBP: electrostatic interactions, adhesion to FBP's planar surface, flocculation by polyvalent cations on FBP's surface, oxidation sterilization from Fe_3O_4 in FBP, irreversible cell structural damage by FBP's edges and corners, and magnetic aggregation under a magnetic field. Thus, FBP is a promising material for effectively treating water with high microbial contamination.

Keywords: magnetic nanoflake; *E. coli* removal; highly salinity water; flocculation; disinfection; recycling

1. Introduction

Microbial contamination of drinking water supplies is a major emerging environmental issue around the world, and even low doses of pathogenic bacteria can pose severe threats to public health, with potentially widespread impacts.[1, 2] As an indicator of fecal contamination, *Escherichia coli* (*E. coli*) is commonly used to evaluate and monitor water quality.[3] Hence, it is common to evaluate the effectiveness of disinfection using the removal efficiency of *E. coli*. There is a need to develop novel biocides, since conventional biocides can become less and less efficient and effective due to the emergence of antibiotic-resistant strains.[4] Recently, a number of new materials or methods have been proposed to remove bacteria from water, for example, polyoxometalate supported ionic liquid phases,[5] single cell imprinting on Ag-ZnO bimetallic nanoparticle modified graphene oxide sheets,[6] silver-modified zeolite,[7] cellulose nanofibers and activated carbon membranes,[8] pompon-like ZnO-PANI heterostructures,[9] electrocoagulation and electro-Fenton[10]. These materials showed removal and/or bactericidal properties. However, developing more sustainable materials for bacterial disinfection is still of great urgency and significance, especially with low cost and easy separation.

It has been proven that Fe_3O_4 nanoparticles (denominated FNPs) generate reactive oxygen species (ROS) when interacting with bacteria, leading to protein oxidation and DNA damage, and finally resulting in cell death [11, 12]. In addition, FNPs can be easily recovered from treated water in the post-treatment using a magnetic field.[1, 11, 13] However, if the FNPs do not possess strong bactericidal property, the aggregates of FNPs that are

not removed could then conceivably serve as anchoring points for further microbial colonization, which would bring up an undesired secondary contamination. Therefore, there has been an increasing number of studies to develop advanced functionalized magnetic nanocomposites for improving removal and disinfection of *E. coli* from contaminated water.[13-16] Magnetic graphene-carbon nanotube iron nanocomposites,[13] magnetic chitosan-graphene oxide composites[12], anti-fimbrial modified magnetic reduced graphene oxide nanoheaters[17], and Ag-$CoFe_2O_4$-GO nano-composites[18] have been reported to be effective adsorbents and antibacterial agents. However, these materials were generally used to purify *E. coli* contaminated water with an initial concentration range of 10^2-10^7 colony forming unit (CFU) per mL, and their removal capacities are limited to $< 10^7$ CFU/mg, which constrains their application range to moderately contaminated water. Furthermore, disinfection of *E. coli* from high-salinity wastewater using these magnetic nanomaterials is limited.

In a previous study we synthesized several types of magnetic phosphate nano-composites by a simple and inexpensive two-step method.[19-22] These materials exhibited high removal efficiency for several dyes (e.g. malachite green, Congo red, methyl blue) from water by hydrogen bonding, ionic interaction, and flocculation. Thus, there is a potential application for removing bacteria by magnetic phosphate nano-composites through similar interactions with different groups outside the cell membrane.

In this work, we applied a novel synthesis approach to prepare magnetic barium phosphate nanoflakes with embedded iron oxide nanoparticles, Fe_3O_4@$Ba_3(PO_4)_2$

(denominated FBP), which possess enhanced saturated magnetization (*Ms*) and surface area compared with our previous work[19]. The removal efficiency of *E. coli* by FBP nanoflakes was evaluated and compared with bare FNPs, in various environmental conditions, including pH, temperature, reaction time, FBP dosage, and initial bacterial concentration, as well as the effects of ionic strength and competitive anions. In addition, the reusability of the FBP nanoflakes was examined through five consecutive bacterial removal cycles. The interactions between *E. coli* and magnetic materials were also investigated in detail by applying several characterization techniques.

2. Experimental

2.1. Materials and reagents

Ferric chloride ($FeCl_3 \cdot 6H_2O$), sodium acetate (NaAc), polyethylene glycol 2000 (PEG 2000), ethylene glycol (EG), barium nitrate, cetyltrimethyl ammonium bromide (CTAB), sodium phosphate, sodium nitrate, sodium sulfate, sodium chloride, nitric acid, and sodium hydroxide were all purchased from Shanghai Sinopharm Chemical Reagent Co., Ltd. (China). All chemicals and reagents were of analytical grade and used as received without any further purification.

2.2. Magnetic barium phosphate synthesis

In the first step, bare black FNPs were prepared using a solvothermal method: 1.35 g $FeCl_3 \cdot 6H_2O$, 1 g PEG 2000, and 3.6 g NaAc were mixed into 40 mL EG by ultrasonic dispersion for 30 min at 30 °C. The mixed solution was transferred into two 50 mL Teflon bottles held in a stainless-steel autoclave, sealed, and maintained at 200 °C for 5 h. After the autoclave cooled to room temperature, the powder was washed with deionized

(DI) water and then with ethanol for five times each. Then, samples were dried in a vacuum oven at 60 °C for 3 h. In the second step, an olive magnetic FBP powder was obtained with the similar process: First, 0.06 g FNPs, 0.01 g CTAB, and 7.5 mmol barium nitrate were ultrasonically dispersed into 40 mL of DI water for 15 min at 30 °C. 5 mmol sodium phosphate was dissolved in 10 mL of DI water and then delivered drop-by-drop slowly into the FNPs/CTAB/$Ba(NO_3)_2$ suspension. CTAB and sodium phosphate were used as versatile soft template and precipitant, respectively. After mechanical stirring for 30 min, the mixed suspension was transferred into two 50 mL Teflon bottles, sealed, heated, cooled, washed, and dried with the same procedure as for the FNPs. At the end of the synthesis, around 1.3 g FBP were obtained at a cost of about \$0.08/g, which indicates the economic efficiency and practicality of this material.

2.3. Characterization

Scanning electron microscopy (SEM) studies were performed on a FEI XL40 Sirion FEG Digital Scanning Microscope with an Oxford energy dispersive spectroscopy (EDS) analysis system. Transmission electron microscope (TEM) image was obtained via a FEI Tecnai G2 Sphera 200 kV Cryo. X-ray diffraction (XRD) patterns were obtained on a Bruker (model AXS D8, Germany) advanced XRD. Specific surface area was measured with a N_2 adsorption isotherm by using an ASAP 2020 M Micromeritics instrument at 100 ^{o}C and via the Brunauer–Emmett–Teller (BET) method. The corresponding zeta potential (ZP) values of the materials were determined via a ZP analyzer (Malvern, Model Nano ZS, England). The magnetic performance of the materials was investigated by a physical property measurement system (PPMS, Model-9, Quantum Design, USA).

The released concentrations of Fe^{3+} and PO_4^{3-} into the solution from materials during the removal process were analyzed with an inductively coupled plasma-atomic emission spectrometry (ICP-AES, Optima 2100, PerkinElmer, USA) and an ion chromatograph (Thermo, model ICS-5000), respectively.

2.4. Bacteria suspension preparation

E. coli was cultivated in 100 mL of Luria Broth (LB) growth medium, consisting of 10 g/L tryptone, 5 g/L bacto-yeast extract, and 10 g/L NaCl. The strain was shaken at 220 rpm and 37 ^{o}C in a thermostatic incubator until the logarithmic growth late phase was reached. Cells were then separated from the growth medium by centrifugation (6000 rpm for 5 min at 15 ^{o}C). The bacterial pellets were washed three times with sterilized DI water to remove the residual growth medium and were then re-suspended in sterilized DI water to obtain bacterial stock solutions with a cell density of approximately 5×10^8 CFU/mL. The concentration of the bacteria suspension was established using the optical density at 600 nm (OD_{600}) measured with a Shimadzu (Japan, model UV1700) ultraviolet spectrophotometer.

2.5. *E. coli* removal

Generally, 0.1 g of either FBP or FNPs was added into 50 mL of *E. coli* suspension (5×10^8 CFU/mL) at 25 °C and pH 6.0 with mechanical stirring for 30 min to investigate the removal efficiency. The pH value was adjusted from 5 to 9 to study its effect on *E. coli* removal efficiency. To investigate the influence of temperature and dosage of material, the studies were done at different temperatures (10, 15, 20, 25, 30, 35, 40 °C) and dosage (0.02 g, 0.05 g, 0.08 g, 0.10 g, 0.15 g). A kinetic study was conducted by

changing the interaction time (2, 5, 10, 20, 30, 40, 50 min). The maximum removal capacity of the magnetic materials (FBP and FNPs) was evaluated via adjusting the initial concentration of *E. coli* ranging from 2.5×10^8 to 12.5×10^8 CFU/mL. A neodymium magnet (diameter of 50 mm, thickness of 5 mm) was used to separate the bacteria-loaded material from aqueous solution, and the residual concentration of *E. coli* was calculated via OD_{600}. To evaluate the reusability of FBP, the bacteria-loaded FBP particles from the first cycle were directly added into the same bacterial suspension to start the next treatment at the same experimental conditions. This was repeated for 5 cycles. All experiment were repeated three times and the average and standard deviation were reported. The interactions between *E. coli* and the magnetic materials were analyzed using optical microscope, SEM, Confocal fluorescent images, and dilution plate count. The related experimental methods are described in the Supporting Information.

3. Results and discussion

3.1. Characterization of materials

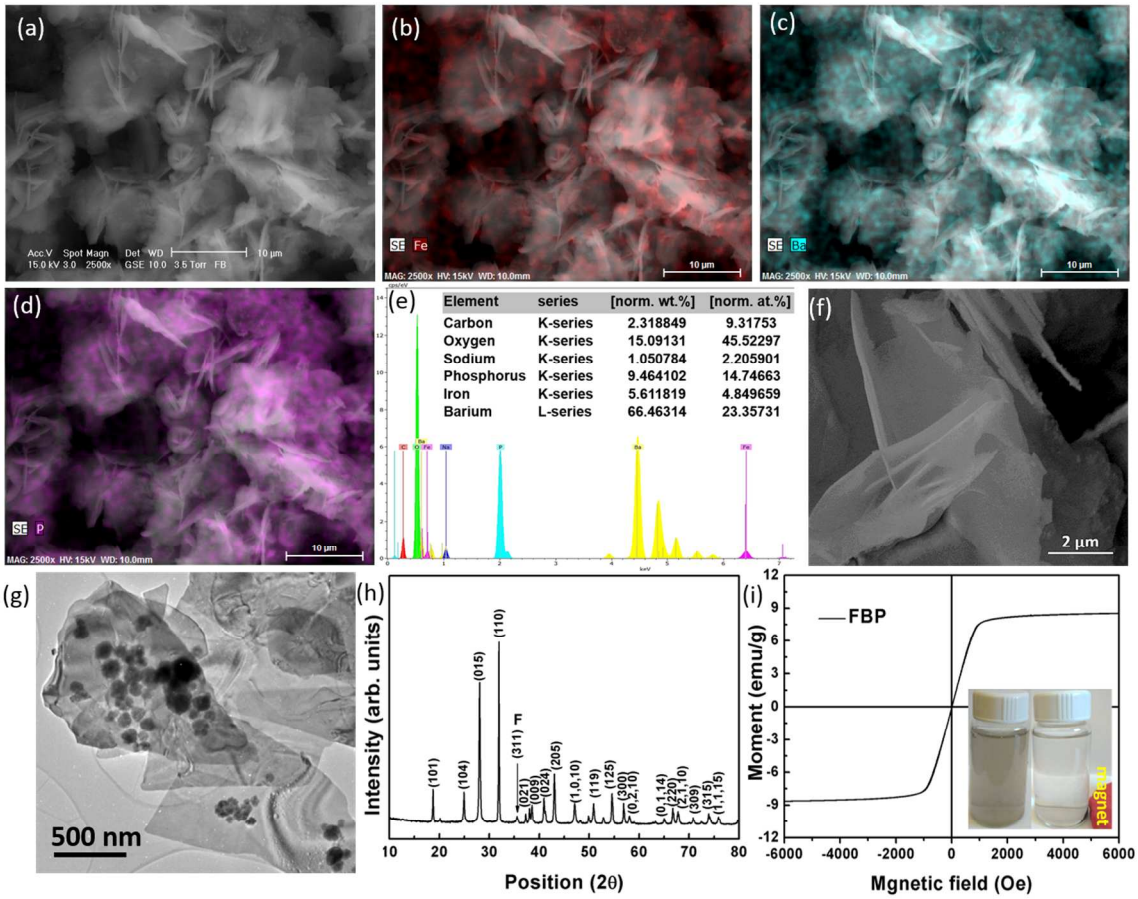

Figure 1. (a) SEM image of FBP; corresponding element mapping of (b) Fe, (c) Ba, and (d) P in FBP; (e) EDS results, (f) SEM close-up of FBP, (g) TEM image of FBP, (h) XRD pattern and (i) magnetic properties of FBP.

As seen from SEM images of FBP (Figures 1a and 1f), FBP exhibits a flake-like structure with the sharp edges and corners. The thickness is around 40 nm and the length is around 7 μm, which is larger than the length of an *E. coli* cell (700 nm-1.2 μm).[18] The plane and large flakes of FBP improve the adhesion of *E. coli* to its surface. EDS results (Figure 1e) demonstrate the presence of Fe, with a content of 4.85% in the FBP nanoflakes. The element mapping results (Figure 1b-d) confirm the uniform distribution of Fe, Ba, and P in the composites. From the EDS X-ray scan, which can go to a depth of

up to 2 μm under the surface, the presence of Fe was uniformly distributed inside the nanoflakes rather than simply adhering physically to the surface or blending into the barium phosphate. This may reduce atmospheric air oxidation and acid corrosion of the embedded FNPs within FBP.[18] The morphology of the FBP nanoflakes was further examined using TEM. Figure 1g shows a thin FBP nanoflake with sharp edges and corners, with embedded FNPs. Pure FNPs possess a spherical shape with an average size of ~100 nm (Figure S1). Hence, FNPs are much smaller than an *E. coli* cell, and they may attach to the *E. coli* cell surface.

On the basis of XRD data (Figure 1h), the main characteristic peaks are attributed to the diffraction of rhombohedral crystal planes of $Ba_3(PO_4)_2$ (JCPDS No. 25-0028).[23] The small peak marked at 35.8° confirmed the presence of Fe with a relatively lower concentration in the composites. The sharp peaks revealed the fine crystallinity of the FBP nano-flakes.[23] As shown in Figure 1i, the magnetic saturation (*Ms*) of FBP is around 8.7 emu/g, which is higher than similar magnetic bactericides[18] and FBP from a previous study with larger iron oxide particles[19]. A strong magnetic response results in easier and faster post-treatment separation, as shown in the embedded picture in Figure 1i. More than 94% of FBP can be separated from water with a small neodymium magnet within 1 min. The surface area of FBP is 48 m^2/g, which is three times higher than the surface area of barium phosphate blended iron oxide submicron particles (14.8 m^2/g) reported previously[19]. This can improve *E. coli* removal because FBP's larger surface area provides more exposed active sites for adhesion.

3.2. Removal of *E. coli* using FBP and FNPs

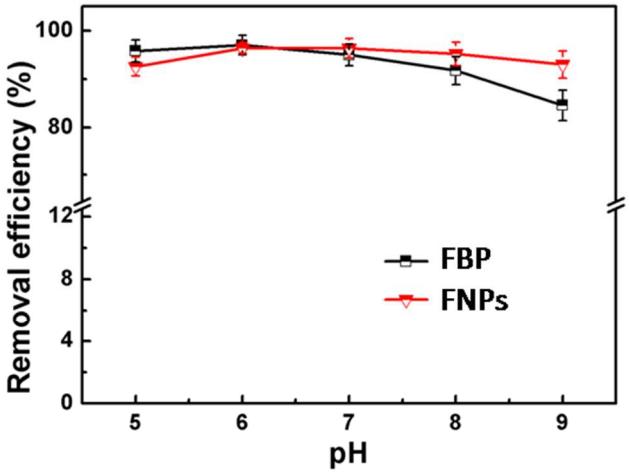

Figure 2. Removal efficiency of *E. coli* (initial concentration, C_0 = 5×10^8 CFU/mL, 25 °C, 30 min) using 2.0 mg/mL of FBP or FNPs at different pH ranging from 5 to 9.

A series of experiments were conducted to investigate the influence of different factors such as temperature, time interval, dosage, initial concentration, and pH on *E. coli* removal using FBP. There was no substantial temperature effect on *E. coli* removal efficiency from 10 °C to 40 °C (Figure S2). Improved removal efficiency was obtained when the FBP dosage was increased from 0.02 g to 0.10 g, while increased initial concentration of *E. coli* led to decreased removal efficiency (Figure S3 and S4). On the basis of optimized treatment conditions, the removal capacity of the FBP nanoflakes (2.43×10^8 CFU/mg) is higher than many previous studies (Table S1), demonstrating high potential of FBP nanoflakes for treating water heavily contaminated with bacteria.

Figure 2 showed the effect of pH on the removal of *E. coli* by FBP and FNPs. Bacterial cells possess a negative surface charge within a pH range of 5.0–9.0,[1] while FBP exhibits a positive ZP at pH < 7 and the isoelectric point of FNPs is slightly above 6 (Figure S5). Thus, the slightly decreased removal efficiency of FBP from 96% to 84% may be due to the change in the particle's surface charge (Figure S5), which implies that

electrostatic interaction is the driving force in the removal process. A similar phenomenon was also reported in a previous study with amine-modified magnetic nanoparticles.[1] The negligible effect of pH on the removal efficiency of FNPs at the tested pH range implies that the electrostatic forces between FNPs and *E. coli* were weak.

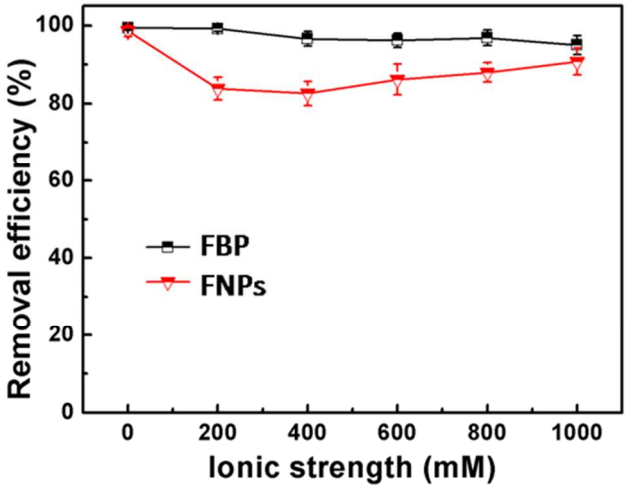

Figure 3. Effect of ionic strength (0-1000 mM NaCl) on *E. coli* removal efficiency (C_0=5×10^8 CFU/mL, 25 °C, pH 6, 30 min) with a dose of 2.0 mg/mL of FBP and FNPs.

The ionic strength of the suspension also influences the surface charge of bacteria and particles, and thus affects the electrostatic interaction between bacterial cells and particle surfaces.[4] As shown in Figure 3, more than 95% of *E. coli* cells could be removed by FBP over the entire range of ionic strength tested (0-1000 mM NaCl), indicating no significant effect was induced by changes in ionic strength. This can be explained by the positive surface charge of FBP over the entire ionic strength range examined (Figure S6) which is beneficial to the attachment of negatively charged *E. coli* onto FBP's surface via electrostatic interaction. Therefore, FBP can be applied to separate bacteria from high-salinity water.

However, the increase in ionic strength from 0 to 400 mM led to the significant

reduction on removal efficiency of FNPs. This is due to a transition of the ZP of FNPs from positive to negative values as ionic strength increases (Figure S6). The enhanced repulsion between *E. coli* and FNPs can result in a decrease in removal efficiency. The gradual increase in the removal efficiency of FNPs at an ionic strength higher than 600 mM (Figure S6) could be ascribed to the decrease in electrostatic repulsion between *E. coli* and FNPs. A similar phenomenon was also reported for interactions between biphasic calcium phosphate ceramic and protein.[24]

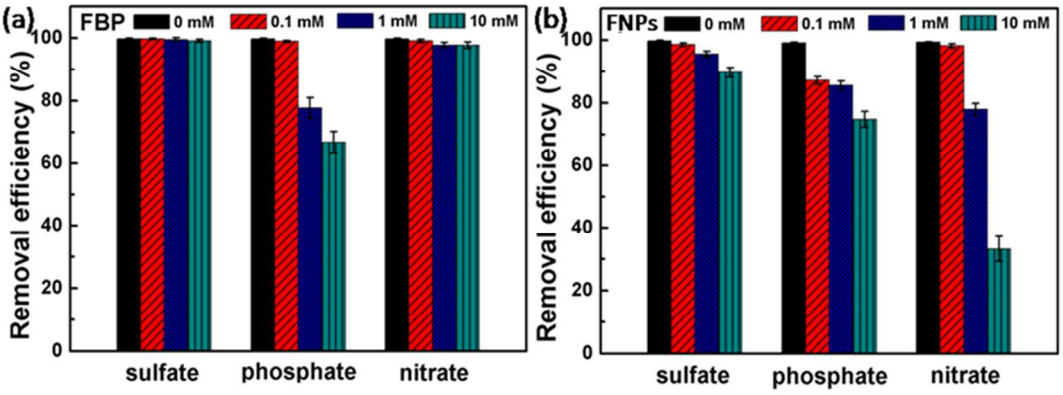

Figure 4. Effect of anions on the removal efficiency of *E. coli* (C_0=5×10^8 CFU/mL, 25 °C, pH 6, 30 min) with a dose of 2.0 mg/mL of (a) FBP and (b) FNPs.

Anions, including sulfate, phosphate, and nitrate are commonly present in surface water and groundwater.[4] These coexisting anions might adsorb onto the surface of the nanomaterials and affect the bacterial attachment process.[25] The typical concentrations of sulfate, phosphate, and nitrate in natural water are usually lower than 10 mM.[26] Therefore, the effects of these anions at a concentration range of 0-10 mM on the bacterial capture efficiency by FBP and FNPs was investigated in this work. As shown in Figure 4, the presence of sulfate and nitrate did not have substantial effects on the removal efficiency of *E. coli* by FBP, while increasing the concentration of phosphate from 0 to 10 mM

decreased FBP's *E. coli* removal ability from 98% to 67%. The ZP of bacteria was negative under all examined conditions regardless of the types of anion or concentration levels.[4] Although the ZP of FBP was influenced by the presence of the anions at difference concentrations (Figure S7), the ZP remained positive at almost all concentrations of sulfate or nitrate, which resulted in a consistent bacterial removal efficiency of FBP in the presence of these anions. Given its large negative charge, phosphate can be easily adsorbed onto the positively charged surface of FBP, leading to a decreased number of active sites on FBP's surface. Therefore, the bacterial removal efficiency of FBP decreased as phosphate concentration increased. For FNPs, the increasing concentration of sulfate, phosphate, or nitrate resulted in decreased removal efficiency of *E. coli*, especially with the addition of nitrate. The adsorbed anions on the surface of FNPs may lead to a major shift in their surface ZP from positive to negative (Figure S7) and enhance the repulsive energy barriers for *E. coli* to attach onto the surface of FNPs. However, it should be noted that the typical concentrations of phosphate and nitrate in natural water are usually below 1 mM.[25] Thus, FBP and FNPs would effectively capture bacterial cells from natural water with the typical concentrations of the coexisting anions.[25] In the case of co-existence of phosphate or nitrite at elevated concentrations, high bacterial removal efficiency may still be obtained by increasing the material dosage (Figure S3).

3.3. Flocculation effect

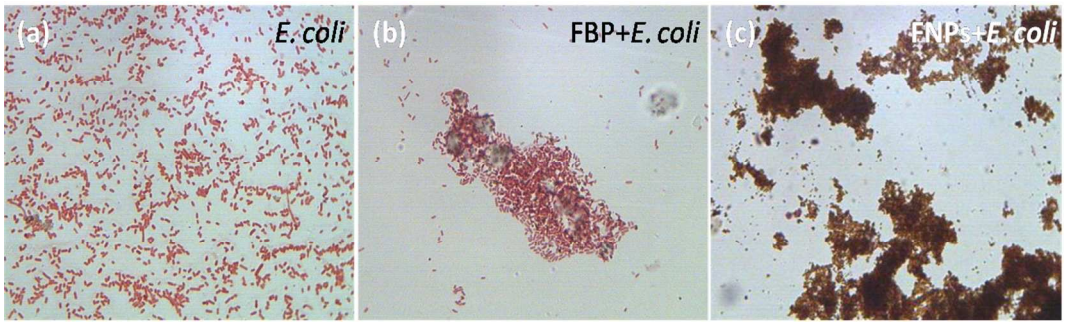

Figure 5. Optical microscope images of (a) pure *E. coli*; *E. coli* adhered to (b) FBP and (c) FNPs after treatment (C_0=5×10^8 CFU/mL, 25 °C, pH 6, material dosage 2.0 mg/mL, 30 min).

In order to understand the interaction between *E. coli* and the magnetic materials, optical microscopy was employed. The images show that pure *E. coli* cells before treatment are dispersed homogeneously (Figure 5a). After being treated with FBP (Figure 5b) and FNPs (Figure 5 c), the bacterial cells aggregated substantially onto the magnetic materials. This was evidenced by the large agglomerates of bacteria (red) and the magnetic materials (black). The surface charge of bacteria is opposite to that of the magnetic materials at pH 6. Therefore, flocs of polyvalent cations on the surface of the magnetic material and the negative cell membrane form rapidly due to charge neutralization, which agrees with previous studies.[4, 27] Importantly, a smaller area of material and larger area of bacteria can be observed in Figure 5b compared with Figure 5c, which implies that FBP is more effective in flocculating *E. coli* than the FNPs. Electrostatic interaction may aid substantially in the flocculation due to charge neutralization.[27] The polyvalent cations on FBP's surface can promote flocculation and accelerate the removal of bacteria.[27, 28] This may be due to the fact that FBP nanoflakes possess more polyvalent cations and more positively charged surfaces than FNPs. It

should be noted that pure $Ba_3(PO_4)_2$ nanoflakes showed a lower removal efficiency (61%) for *E. coli* (Figure S8) than FBP though they shared a similar shape and surface area.[23] Therefore, the flocculation effect from the iron in FBP (e.g. iron nanoparticles, iron ions, iron oxides, and hydrolysis products) contribute to *E. coli* removal.[27, 28] Furthermore, PO_4^{3-} groups associated with FBP can combine with H^+ to help release Fe^{3+} and Fe^{2+}; this can increase the flocculation effect of FBP as hydrolysis products (e.g. $[Fe(OH)]^{2+}$, $[Fe(OH)_2]^+$, $[Fe(OH)]^+$) can also produce agglomeration of microorganisms[27].

3.4. Reuse of FBP and FNPs

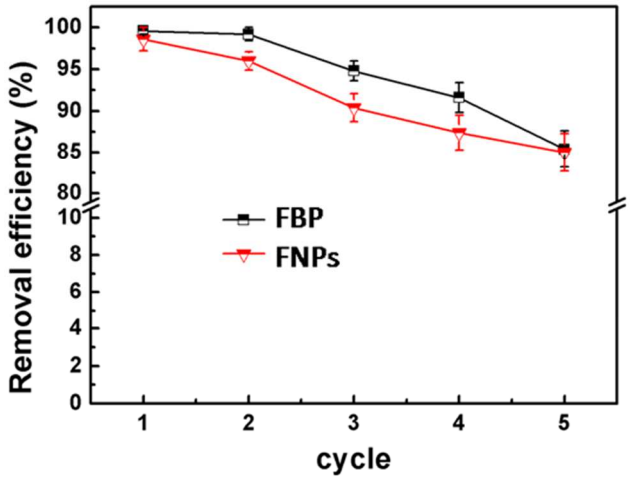

Figure 6. Removal efficiency of *E. coli* at different cycles (C_0=5×10^8 CFU/mL, 25 °C, pH 6, 30 min) with an initial dosage of 2.0 mg/mL FBP and FNPs.

The recovery and reuse of FBP and FNPs throughout five consecutive bacteria removal experiments are illustrated in Figure 6. It can be observed that the *E. coli* removal efficiencies of both FBP and FNPs were more than 90% in the first cycle, and then decreased slowly after each cycle. This tendency can be explained by the fact that the materials were covered by more bacteria after additional cycles, which can result in decreased surface charge from positive to negative values (Figure S9) and less sites

available for other bacterial attachment. However, FBP still removes around 87% of *E. coli* after five cycles and FNPs remove 86% under the same conditions. Thus, the electrostatic interaction may be not the dominant mechanism for the high removal efficiency during the reuse.

The chemical stability of the magnetic materials and the retention of adsorbed bacteria are significant in the reuse process to avoid secondary pollution (from the release of components of the FBP, FNPs or bacteria) to the treated water.[18] On the basis of ICP-AES and ion chromatography analysis, there was no significant release of Fe^{3+} or PO_4^{3-} to the solution from the magnetic materials during five cycles, which demonstrates the chemical stability of FBP and FNPs in the removal process. After bacterial treatment, the FBP and FNPs were rinsed with 50 mL of sterilized DI water three times to determine whether the captured bacteria on the surface of these materials could be released back into the environment, resulting in secondary pollution. On the basis of dilution plate count results (Figure S10), FBP that had been loaded with bacteria released less live *E. coli* (0.48%) into solution than FNPs (0.96%). This may be due to the stronger electrostatic binding and flocculation by FBP or better disinfection effect by FBP. Furthermore, after being rinsed ultrasonically for 5 min, FBP acquired a positive surface charge again, which implies that the captured cells were washed off and the materials could be reused.

3.5. Disinfection effect

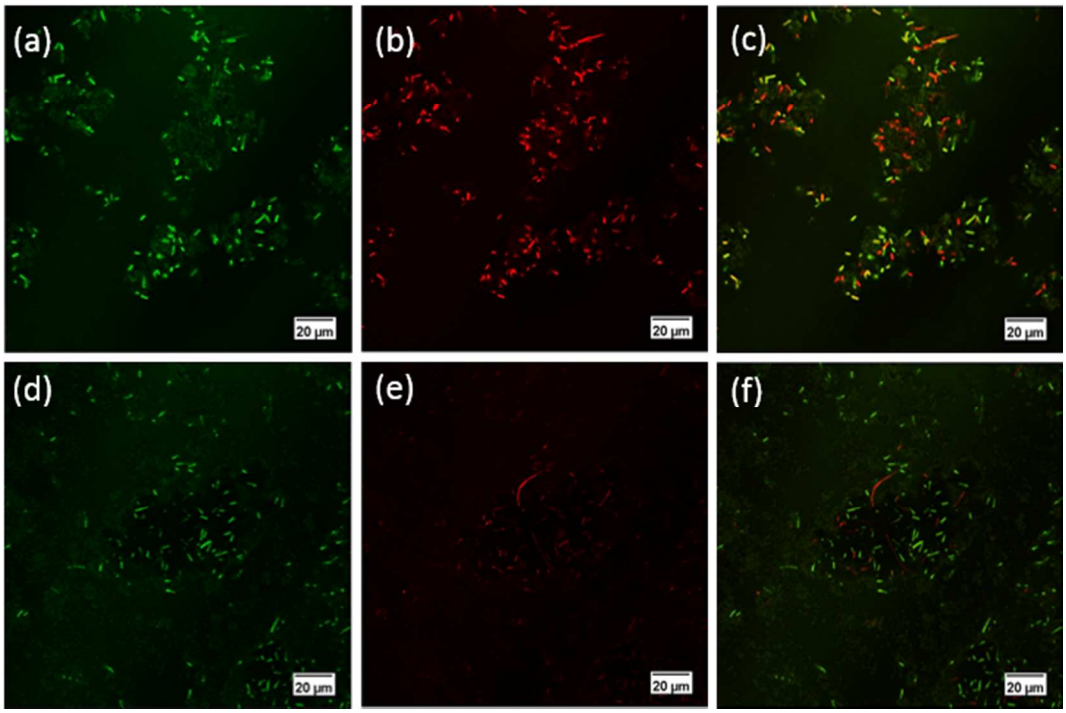

Figure 7. Confocal fluorescent images of live and dead bacterial cells treated with FBP (a−c) and FNPs (d−f) under mechanical stirring and stained with SYTO9 (green) and PI (red). (c, f) Overlying images of *E. coli* stained with SYTO9 (live and dead) and PI (dead).

In order to confirm whether the cells were affected by the magnetic materials in a reversible manner or not, fluorescent-based cell tests of live and dead bacterial cells were conducted (Figure 7). The strong green fluorescence intensity region (Figure 7a and d) represents the proportion of live and dead bacteria, and the heavy red fluorescence intensity region (Figure 7b and e) indicates the dead fraction.[18] It can be clearly observed from Figure 7b that most of the bacteria adhered to FBP's surface are dead, indicating irreversibly damaged cell membranes or mass cell death upon exposure to FBP.[3] However, most of bacteria cells were still alive after being treated with FNPs (Figure 7d and e).

Removal kinetics are shown in Figure S11 and S12. Maximum removal was achieved after 30 min, with no substantial improvement with longer times. The kinetics behavior of the disinfection process was determined by considering the disinfection at different time intervals; the confocal fluorescent images were used to evaluate the ratio of live and dead bacterial cells treated with FBP and FNPs. As shown in Figure S13, around 30%, 70%, and 90% of bacteria were inactivated after treatment with FBP under shaking for 5 min, 10 min, and 30 min, respectively. However, FNPs showed a lower disinfection ratio (less than 40%) after 30 min (Figure S14) under shaking compared with FBP under shaking (Figure S13).

FBP under mechanical stirring (Figure 7) or shaking (Figure S13g-i) generated a similar disinfection effect, implying that the stirring paddle itself was not likely the cause of cell death. Furthermore, without any mechanical mixing, FBP resulted in much lower disinfection (less than 20%) (Figure S15) than FBP under mechanical stirring (Figure 7) or shaking (Figure S13). This implies that the mechanical mixing process can improve FBP's physical bactericidal action because it allows more bacteria to contact the sharp FBP nanoflake edges. The pure cations (Fe^{2+}, Fe^{3+}, or Ba^{2+}) showed no noticeable toxicity to *E. coli* (Figure S16). Once the cell membrane is broken by FBP, ROS or some cations in solution can react with protein, DNA, or other matters inside the cell, leading to cell death.

Dilution plate count assay was conducted to measure cell proliferation after treatment with FBP and FNPs (Figure S17). Cell proliferation was weakest for the treatment using FBP under stirring, which is consistent with confocal fluorescent results. To further

investigate the underlying mechanism and inspect the bacterial morphological change, *E. coli* cells adhered with FBP and FNPs were visualized using SEM. Compared with pure *E. coli* (Figure S18a), most of the bacterial cells fused onto the FBP surface with an irregular shape (Figure S18b) which seemed to exhibit a plasmolysis phenomenon[18, 28]. Only a small number of *E. coli* cells were found fixed onto the FBP plane (Figure S18c and d). But some of the cell membranes were deformed from the normal rods to round shapes. Similar results were seen in other antibacterial materials, such as magnetic chitosan-graphene oxide composite and graphene-based antibacterial paper[12, 29]. The leakage of intracellular constituents and change of morphology may be due to altered cell permeability resulting from the interaction between positively charged FBP and the negatively charged membrane of cells[30]. Moreover, iron oxide nanoparticles have been shown to generate ROS when interacting with bacteria, resulting in protein oxidation and cell death[31,32]. Additionally, *E. coli* cells were observed to be divided into two parts after contacting the sharp FBP edge (Figure S18e and f), demonstrating physical damage.

It was interesting to note that the FNPs aggregated and adhered to some of the *E. coli* cells, forming pits on the bacterial surface and leading to irregular shapes (Figure S18g-i). This implies that adhesion of FNPs onto the surface of *E. coli* may cause destruction of cell integrity, similar to other materials[13, 33]. Although the FNPs may lead to disinfection via oxidation, the small spherical structure of FNPs with low positive charge may result in weaker adhesion, piercing, or other physical action to bacteria cells compared with FBP. Although the FNPs may lead to disinfection via oxidation, the small spherical structure of FNPs with low positive charge may result in weaker adhesion, piercing, or

other physical action to bacteria cells compared with FBP.

4. Conclusions

In this study, magnetic FBP nanoflakes were synthesized, to be used for disinfection and removing bacteria from contaminated waters. The bacterial removal efficiency of FBP was systematically studied compared with bare FNPs. Results showed that FBP could remove 97% of *E. coli* at the optimized experimental conditions (initial concentration of 5×10^8 CFU/mL, pH=6, 25 °C, reaction time of 30 min, material dosage of 2 mg/mL). FBP was still an effective disinfectant even in high salinity waters and in the presence of common anions at concentrations typical of most water sources. Moreover, 87% of *E. coli* cells could be removed by FBP even in the fifth reuse cycle, demonstrating good reusability. FBP performs better as a disinfectant than FNPs due to its composition and morphology: (1) the higher positive charge of FBP due to the addition of barium phosphate to FNPs improves electrostatic interactions, altering cell permeability and inducing plasmolysis; (2) the special two-dimensional flake structure of FBP with sharp edges and corners can induce the physical disruption of the bacterial cell membrane, releasing cellular components, and resulting in cell death, similar to magnetic graphene[34]. The removal and disinfection mechanisms of FBP inlcude: electostatic adhesion onto surface, flocculation effect of polyvalent cations, oxidation inactivation by Fe_3O_4 in FBP, irreversible cell damage by FBP's sharp structure. Cell damage from the sharp edges was confirmed the low disinfection when FBP is added without mechanical mixing or stirring; shaking or stirring of FBP resulted in similarly high disinfection via cell damage. Generally, taking into account the easy preparation, magnetic separation,

high removal efficiency, effective disinfection, and good reusability, magnetic FBP nanoflakes are an ideal material for water disinfection.

Conflicts of interest

There are no conflicts to declare.

Acknowledgements

This work was financially supported by the Jiangsu Natural Science Funds of China (Grant No. SBK2017020336), the Fundamental Research Funds for the Central Universities (Grant No. KYZ201747), and the National Natural Science Funds of China (Grant No. 51402153). This work was in part supported by the National Science Foundation (NSF) and the U.S. Environmental Protection Agency (EPA) under NSF-EF0830117. Any opinions, findings, conclusions or recommendations expressed in this material are those of the authors do not necessarily reflect the views of the funding agencies.

Electronic supplementary information

(1) Characterization experiment methods: Optical microscope, Fluorescent-based cell live/dead test, SEM of *E. coli* with material, and Dilution plate count method; (2) Effects of temperature, interaction time, dosage, and initial *E. coli* concentration on bacterial removal; (3) Comparisons of removal capacity for *E. coli* by per mg material in this work with other recent reports; (4) Zeta potentials of FBP and FNPs at different pH, ionic strength, co-exiting anions, and cycle; (5) Bacterial removal effect of rare barium phosphate nanoflake; (6) Dilution plating procedure results; (7) Kinetics of removal and disinfection process by FBP and FNPs; (8) Confocal fluorescent images of *E. coli* cells

treated in solutions containing metal ions leased from FBP; (9) Cell proliferation after treatment by FBP and FNPs, and (10) SEM images of *E. coli* with FBP and FNPs treatment after magnetic separation.

References

1. S. Zhan, Y. Yang, Z. Shen, J. Shan, Y. Li, S. Yang and D. Zhu, Efficient removal of pathogenic bacteria and viruses by multifunctional amine-modified magnetic nanoparticles, *Journal of hazardous materials*, 2014, **274**, 115-123.
2. S. Singh, K. Barick and D. Bahadur, Inactivation of bacterial pathogens under magnetic hyperthermia using Fe 3 O 4–ZnO nanocomposite, *Powder Technology*, 2015, **269**, 513-519.
3. S. Zhan, D. Zhu, S. Ma, W. Yu, Y. Jia, Y. Li, H. Yu and Z. Shen, Highly efficient removal of pathogenic bacteria with magnetic graphene composite, *ACS applied materials & interfaces*, 2015, **7**, 4290-4298.
4. Y. Jin, F. Liu, C. Shan, M. Tong and Y. Hou, Efficient bacterial capture with amino acid modified magnetic nanoparticles, *Water research*, 2014, **50**, 124-134.
5. S. Herrmann, L. De Matteis, J. M. de la Fuente, S. G. Mitchell and C. Streb, Removal of Multiple Contaminants from Water by Polyoxometalate Supported Ionic Liquid Phases (POM-SILPs), *Angewandte Chemie International Edition*, 2017, **56**, 1667-1670.
6. E. Roy, S. Patra, A. Tiwari, R. Madhuri and P. K. Sharma, Single cell imprinting on the surface of Ag–ZnO bimetallic nanoparticle modified graphene oxide sheets for targeted detection, removal and photothermal killing of E. Coli, *Biosensors and Bioelectronics*, 2017, **89**, 620-626.
7. L. Akhigbe, S. Ouki and D. Saroj, Disinfection and removal performance for Escherichia coli and heavy metals by silver-modified zeolite in a fixed bed column, *Chemical Engineering Journal*, 2016, **295**, 92-98.
8. M. Hassan, R. Abou-Zeid, E. Hassan, L. Berglund, Y. Aitomäki and K. Oksman, Membranes based on cellulose nanofibers and activated carbon for removal of Escherichia coli bacteria from water, *Polymers*, 2017, **9**, 335.
9. T. Zou, C. Wang, R. Tan, W. Song and Y. Cheng, Preparation of pompon-like ZnO-PANI heterostructure and its applications for the treatment of typical water pollutants under visible light, *Journal of Hazardous Materials*, 2017, **338**, 276-286.
10. E. Anfruns-Estrada, C. Bruguera-Casamada, H. Salvadó, E. Brillas, I. Sirés and R. M. Araujo, Inactivation of microbiota from urban wastewater by single and sequential electrocoagulation and electro-Fenton treatments, *Water research*, 2017, **126**, 450-459.
11. S. Singh, K. Barick and D. Bahadur, Fe 3 O 4 embedded ZnO nanocomposites for the removal of toxic metal ions, organic dyes and bacterial pathogens, *Journal of Materials Chemistry A*, 2013, **1**, 3325-3333.
12. Y. Jiang, J.-L. Gong, G.-M. Zeng, X.-M. Ou, Y.-N. Chang, C.-H. Deng, J. Zhang, H.-Y. Liu and S.-Y. Huang, Magnetic chitosan–graphene oxide composite for anti-microbial and dye removal applications, *International journal of biological macromolecules*, 2016, **82**, 702-710.
13. V. K. Sharma, T. J. McDonald, H. Kim and V. K. Garg, Magnetic graphene–carbon nanotube iron nanocomposites as adsorbents and antibacterial agents for water purification, *Advances in colloid and interface science*, 2015, **225**, 229-240.
14. K. Niemirowicz, I. Swiecicka, A. Z. Wilczewska, K. H. Markiewicz, U. Surel, A. Kułakowska, Z. Namiot, B. Szynaka, R. Bucki and H. Car, Growth arrest and rapid capture of select pathogens following magnetic nanoparticle treatment, *Colloids and Surfaces B: Biointerfaces*, 2015, **131**, 29-38.
15. S. Chella, P. Kollu, E. V. P. Komarala, S. Doshi, M. Saranya, S. Felix, R. Ramachandran, P.

Saravanan, V. L. Koneru and V. Venugopal, Solvothermal synthesis of MnFe 2 O 4-graphene composite—Investigation of its adsorption and antimicrobial properties, *Applied Surface Science*, 2015, **327**, 27-36.

16. J. Chen, B. Duncan, Z. Wang, L.-S. Wang, V. M. Rotello and S. R. Nugen, Bacteriophage-based nanoprobes for rapid bacteria separation, *Nanoscale*, 2015, **7**, 16230-16236.
17. F. Halouane, R. Jijie, D. Meziane, C. Li, S. K. Singh, J. Bouckaert, J. Jurazek, S. Kurungot, A. Barras and M. Li, Selective isolation and eradication of E. coli associated with urinary tract infections using anti-fimbrial modified magnetic reduced graphene oxide nanoheaters, *Journal of Materials Chemistry B*, 2017, **5**, 8133-8142.
18. S. Ma, S. Zhan, Y. Jia and Q. Zhou, Highly efficient antibacterial and Pb (II) removal effects of Ag-CoFe2O4-GO nanocomposite, *ACS applied materials & interfaces*, 2015, **7**, 10576-10586.
19. F. Zhang, X. Yin, J. Lan and W. Zhang, Application of Ba3 (PO4) 2/Fe3O4 as a novel magnetic adsorbent to remove methyl blue from aqueous solution, *Journal of materials science*, 2016, **51**, 3525-3535.
20. F. Zhang, X. Yin and W. Zhang, Development of magnetic Sr 5 (PO 4) 3 (OH)/Fe 3 O 4 nanorod for adsorption of Congo red from solution, *Journal of Alloys and Compounds*, 2016, **657**, 809-817.
21. F. Zhang, B. Ma, X. Jiang and Y. Ji, Dual function magnetic hydroxyapatite nanopowder for removal of malachite green and Congo red from aqueous solution, *Powder Technology*, 2016, **302**, 207-214.
22. F. Zhang, Z. Wei, W. Zhang and H. Cui, Effective adsorption of malachite green using magnetic barium phosphate composite from aqueous solution, *Spectrochimica Acta Part A: Molecular and Biomolecular Spectroscopy*, 2017, **182**, 116-122.
23. F. Zhang, Z. Zhao, R. Tan, Y. Guo, L. Cao, L. Chen, J. Li, W. Xu, Y. Yang and W. Song, Selective and effective adsorption of methyl blue by barium phosphate nano-flake, *Journal of colloid and interface science*, 2012, **386**, 277-284.
24. X. Zhu, H. Fan, D. Li, Y. Xiao and X. Zhang, Protein adsorption and zeta potentials of a biphasic calcium phosphate ceramic under various conditions, *Journal of Biomedical Materials Research Part B: Applied Biomaterials*, 2007, **82**, 65-73.
25. Y. Jin, J. Deng, J. Liang, C. Shan and M. Tong, Efficient bacteria capture and inactivation by cetyltrimethylammonium bromide modified magnetic nanoparticles, *Colloids and Surfaces B: Biointerfaces*, 2015, **136**, 659-665.
26. L. C. Roberts, S. J. Hug, T. Ruettimann, M. M. Billah, A. W. Khan and M. T. Rahman, Arsenic removal with iron (II) and iron (III) in waters with high silicate and phosphate concentrations, *Environmental Science & Technology*, 2004, **38**, 307-315.
27. M. W. Tenney and W. Stumm, Chemical flocculation of microorganisms in biological waste treatment, *Journal (Water Pollution Control Federation)*, 1965, **37**, 1370-1388.
28. E. Neyens and J. Baeyens, A review of thermal sludge pre-treatment processes to improve dewaterability, *Journal of hazardous materials*, 2003, **98**, 51-67.
29. W. Hu, C. Peng, W. Luo, X. Li, D. Li, Q. Huang and C. Fan, Graphene-Based Antibacterial Paper, *ACS Nano*, 2010, **4**, 4317-4323.
30. E. I. Rabea, M. E. T. Badawy, C. V. Stevens, G. Smagghe and W. Steurbaut, Chitosan as Antimicrobial Agent: Applications and Mode of Action, *Biomacromolecules*, 2003, **4**, 1457-1465.
31. N. Tran, A. Mir, D. Mallik, A. Sinha, S. Nayar and T. J. Webster, Bactericidal effect of iron oxide nanoparticles on Staphylococcus aureus, *International Journal of Nanomedicine*, 2010, **5**, 277-283.

32. B. Stephen Inbaraj, T. Y. Tsai and B. H. Chen, Synthesis, characterization and antibacterial activity of superparamagnetic nanoparticles modified with glycol chitosan, *Science and Technology of Advanced Materials*, 2012, **13**, 015002.

33. S. Singh, K. Barick and D. Bahadur, Surface engineered magnetic nanoparticles for removal of toxic metal ions and bacterial pathogens, *Journal of Hazardous Materials*, 2011, **192**, 1539-1547.

34. G. Gollavelli, C.-C. Chang and Y.-C. Ling, Facile synthesis of smart magnetic graphene for safe drinking water: heavy metal removal and disinfection control, *ACS Sustainable Chemistry & Engineering*, 2013, **1**, 462-472.

Table of Contents

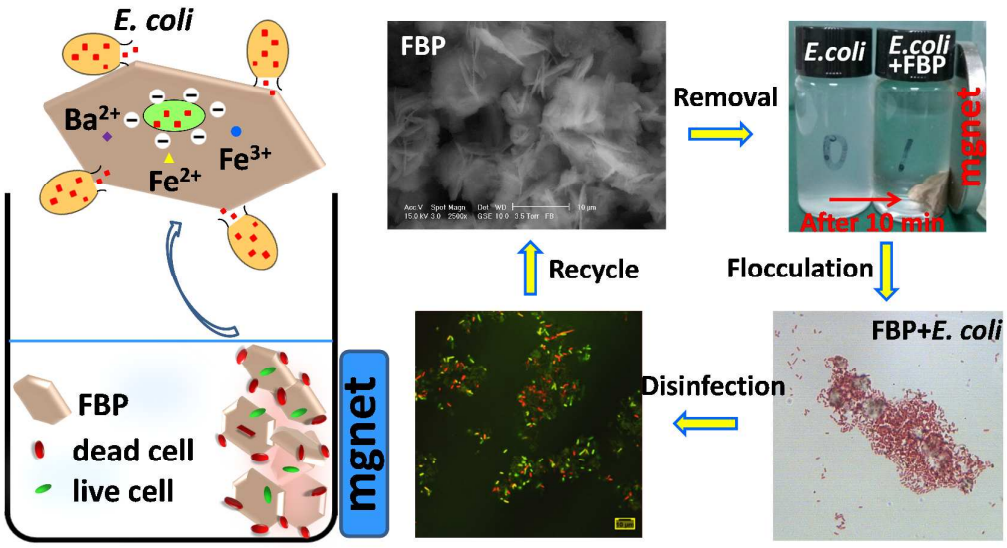

Highly efficient bacterial removal and disinfection of drinking water by recyclable magnetic barium phosphate nanoflakes with embedded iron oxide nanoparticles